Published in final edited form as:
Cancer Res. 2008 May 1; 68(9): 3185–3192. doi:10.1158/0008-5472.CAN-07-2673.

Fibronectin Expression Modulates Mammary Epithelial Cell Proliferation during Acinar Differentiation

Courtney M. Williams, **Adam J. Engler**, **R. Daniel Slone**, **Leontine L. Galante**, and **Jean E. Schwarzbauer**
Department of Molecular Biology, Princeton University, Princeton, New Jersey

Abstract

The mammary gland consists of a polarized epithelium surrounded by a basement membrane matrix that forms a series of branching ducts ending in hollow, sphere-like acini. Essential roles for the epithelial basement membrane during acinar differentiation, in particular laminin and its integrin receptors, have been identified using mammary epithelial cells cultured on a reconstituted basement membrane. Contributions from fibronectin, which is abundant in the mammary gland during development and tumorigenesis, have not been fully examined. Here, we show that fibronectin expression by mammary epithelial cells is dynamically regulated during the morphogenic process. Experiments with synthetic polyacrylamide gel substrates implicate both specific extracellular matrix components, including fibronectin itself, and matrix rigidity in this regulation. Alterations in fibronectin levels perturbed acinar organization. During acinar development, increased fibronectin levels resulted in overproliferation of mammary epithelial cells and increased acinar size. Addition of fibronectin to differentiated acini stimulated proliferation and reversed growth arrest of mammary epithelial cells negatively affecting maintenance of proper acinar morphology. These results show that expression of fibronectin creates a permissive environment for cell growth that antagonizes the differentiation signals from the basement membrane. These effects suggest a link between fibronectin expression and epithelial cell growth during development and oncogenesis in the mammary gland.

Introduction

The cellular microenvironment, specified by cell-cell and cellextracellular matrix (ECM) interactions, is crucial for regulating the development, maintenance, and functionality of cells within tissues (1). In cancer, the microenvironment plays a central role in disease progression. Normal ECM cues can quench tumorigenic properties of cells as shown by the regulated clonal growth of oncogenic v-src–transformed cells in normal chick embryos (2). On the other hand, environmental conditions can also promote tumor formation, such as that which occurred in mice after coinjection of nontumorigenic epithelial cells with fibroblasts from malignant tumors (3). In breast and other cancers, histologically normal tissues adjacent to tumors have been found to harbor the same genetic abnormalities as the tumor cells (4,5), further supporting the notion that the microenvironment contributes to oncogenic phenotypes. Therefore, to understand cancer progression, the effects of molecules that direct cell responses within the microenvironment must be identified.

The ECM governs a wide variety of cellular processes, including proliferation, differentiation, and migration, and changes in the ECM microenvironment occur during both developmental

Requests for reprints: Jean E. Schwarzbauer, Princeton University, Department of Molecular Biology, Washington Road, Princeton, NJ 08544-1014. Phone: 609-258-2893; Fax: 609-258-1035; E-mail: jschwarz@princeton.edu.

and disease processes (6,7). The mammary gland provides an excellent example of these changes, as ECM composition is modulated during development (8) and oncogenesis (9). The normal mammary gland consists of a series of branching ducts, each branch ending with an acinus, which has a hollow, sphere-like structure and is the functional unit of the mammary gland responsible for milk secretion. Each acinus is composed of a single layer of polarized mammary epithelial cells surrounded by a basement membrane of collagens I, III, and IV, laminin, and heparan sulfate proteoglycans (10).

Mammary gland development and breast oncogenesis are accompanied by dramatic alterations in the composition, architecture, and mechanical properties of the ECM. During development, as branching morphogenesis occurs, levels of fibronectin, laminin, and collagen I increase, with fibronectin showing the most dramatic changes (8). Epithelial cell–associated fibronectin also increases as the mammary gland prepares for lactation (8). During oncogenesis, the basement membrane is not maintained and its components are distributed throughout the tumor stroma (9). Compositionally, there are changes in deposition of certain matrix proteins within tumors, including elastin, tenascin-C, osteopontin, collagen III, and fibronectin (11–14). Mechanically, these alterations to the matrix result in an increase in the rigidity of the mammary tissue to levels capable of perturbing the morphology and proliferative state of mammary epithelial cells *in vitro* (15,16). The signals responsible for these changes in ECM composition, as well as subsequent cellular responses, are an area of active research.

In normal adult mammary tissue, interstitial ECM is largely devoid of fibronectin (14) and the tissue is soft and pliable (15). However, increased fibronectin levels have been observed in the stroma of benign hyperplasias and various types of mammary tumors (13,14) and established tumor tissue has a stiffness that is an order of magnitude higher than normal tissue (17). Histologic data are supported by reverse transcriptase–PCR (RT-PCR) and microarray analyses of transcript levels showing an up-regulation of fibronectin associated with primary malignancies (12,18). This matrix abnormality seems to affect disease outcome, as high fibronectin and β1 integrin levels in tumor sections correlate with decreased survival of breast cancer patients (19). These studies provide circumstantial evidence for a role for fibronectin in the development and/or progression of mammary tumorigenesis. However, the mechanisms by which fibronectin expression is controlled and its molecular contributions to the early stages of breast cancer pathology have yet to be uncovered.

To address this issue, we are using a well-established culture system, in which mammary epithelial cells are induced to differentiate on a three-dimensional Matrigel reconstituted basement membrane matrix (20). Morphogenesis of nontumorigenic MCF-10A cells on this matrix recapitulates an acinar morphology similar to normal mammary tissue (Fig. 1*A*). In early, proliferative stages of differentiation, single cells grow into multicellular clusters and initiate secretion of basement membrane components, such as type IV collagen and laminin-5 (20,21). Subsequently, the outer layer of cells becomes polarized to the basement membrane and cell growth is arrested. The interior cells then undergo apoptosis resulting in a hollow acinus (22,23). Thus, well-developed acini are characterized by a hollow lumen surrounded by a single layer of growth-arrested cells.

It has been known for some time that signaling from ECM is crucial for acinar development. In the three-dimensional culture system, laminin-1 plays a key role in establishing epithelial cell polarity (24). Function-blocking antibodies targeting the β1 integrin subunit perturb acinar morphogenesis (21,25), and these effects have been attributed to laminin-binding receptors. Fibronectin also signals through β1 integrins, but its contribution to acinar morphogenesis has not been directly addressed. Moreover, ECM protein composition determines matrix rigidity, a property that has recently been implicated in control of mammary epithelial morphogenesis. Increasing the stiffness of the growth substrate from normal physiologic levels (~0.15 kPa) to

pathologic levels found in tumors (~4.0 kPa) prevented mammary epithelial cells from forming acini (17). We show here that fibronectin expression is modulated by matrix composition and rigidity during acinar morphogenesis and that excess fibronectin affects the proliferative state of MCF-10A cells in acinar cultures with significant effects on acinar size.

Materials and Methods

Cell culture

MCF-10A cells were obtained from the American Type Culture Collection and cultured as previously described (20). Cells were cultured for no more than 30 passages.

Three-dimensional basement membrane culture

Morphogenesis assays were conducted as previously described (20), except cells were plated at 2,500 per well in eight-well Nunc chamber slides. Rat plasma fibronectin in CAPS buffer [10 mmol/L CAPS (pH 11), 150 mmol/L NaCl] was added to either culture medium (at 50–100 μg/mL) or Matrigel matrix (at 25 μg/mL). Control cultures received the equivalent amount of CAPS buffer. Assay medium is 2% horse serum, which contributes ~0.6 Ag fibronectin/mL of medium. Rat plasma fibronectin was purified from rat plasma (Taconic) by gelatin-Sepharose affinity chromatography as previously described (26).

Immunofluorescence microscopy

Immunofluorescence staining of acini was done as previously described by Debnath et al. (20). Visualization was done using a Nikon TE2000U microscope equipped with a Cooke SensiCam^{QE} High-Performance Camera and CARV spinning-disc confocal (Atto Biosciences). Images were acquired and managed using IPLab software. Fibronectin levels in acini were determined by measuring the average fluorescence intensity per pixel along both the *x* and *y* diameters of the widest confocal cross-section of each antifibronectin-stained acinus using unmodified images captured with equal exposure times.

Primary antibodies include antihuman fibronectin HFN 7.1 culture supernatant at 1:500 (Developmental Studies Hybridoma Bank) and anti– Ki-67 at 1:150 (Zymed). HFN7.1 is species-specific and does not recognize mouse fibronectin (27). Secondary Alexa Fluor goat anti-mouse and goat anti-rabbit antibodies (Molecular Probes) were used at 1:300. Other reagents include Alexa Fluor 488–conjugated phalloidin and rhodamine-phalloidin, both at 1:500 (Molecular Probes) and 4′,6-diamidino-2-phenylindole (DAPI; Sigma-Aldrich) at 0.75 μg/mL.

To assess acinar size and morphology, cultures were fixed and stained with DAPI, fluorescently conjugated phalloidin, and antibodies against Ki-67 as indicated. By confocal microscopy, the widest cross-section of each acinus was located and examined, excluding only those acini in direct contact with neighbors. In each cross-section, the total number of cells, the number of Ki-67 positive cells, the number of cells lining the circumference, and the number of cells in the interior were counted. Only nuclei clearly in the plane of focus were counted. A hollow acinus was defined as one lacking any nuclei in the interior of the structure. To visualize the size distribution of the population, acini were grouped by cell number into bins of four cells, the frequency of occurrence was graphed, and the distribution was fitted with a Gaussian curve. To determine the significance of size differences between acini grown on Matrigel (control) versus Matrigel with fibronectin, the average number of cells per acinus was calculated for the control and the percentage of acini with more cells than the control average was determined and graphed. The statistical significance of the percentages was determined using a *t* test of proportions (see Statistical analysis in Materials and Methods).

Metabolic labeling and quantification of fibronectin production

Cells were cultured for the indicated periods of time, in the absence or presence of excess fibronectin, at a concentration of 50 μg/mL and labeled with 100 μCi [^{35}S]methionine (MP Biomedicals)/mL of medium for 24 h before collection of the medium and lysis of cells in modified RIPA buffer (28). Fibronectin was isolated from culture medium using gelatin-Sepharose binding (26). Isolated fibronectin was then reduced by addition of 0.1 mol/L DTT and separated by SDS-PAGE. Gels were dried, placed on a phosphor storage screen and bands detected and quantified using a Storm 860 system (GE Healthcare Life Sciences). Samples were normalized before loading using results from a β-*N*-acetylglucosaminidase activity assay (Sigma) performed on cell lysates.

Polyacrylamide substrates

Polyacrylamide substrates were made as previously described (29,30). Briefly, polyacrylamide gels were polymerized on aminosilanized glass coverslips. To modulate the stiffness of the gel, the acrylamide to cross-linker *N*,*N*′ methylene-*bis*-acylamide ratio was varied as follows: 3% to 0.06% acrylamide/*bis*-acrylamide for 0.3 kPa, 4% to 0.15% acrylamide/*bis*-acrylamide for 3.5 kPa, and 10% to 0.3% acrylamide/*bis*-acrylamide for 34 kPa. Laminin-1 (kindly provided by Dr. Peter Yurchenco, Robert Wood Johnson Medical School) or fibronectin were attached to the gel surfaces using a photo-activated bifunctional cross-linker sulfo-SANPAH (Pierce) and 10 μg/mL protein solutions in 50 mmol/L HEPES (pH 8.5).

Cells were plated in assay medium on polyacrylamide gels with different elastic moduli at 12×10^4 cells per well in a 24-well dish for 24 h, at which time gels were transferred to new wells and metabolic labeling was done as described above.

Real-time RT-PCR

MCF-10A cells were plated in wells of a 24-well dish at 12×10^4 cells per well with or without Matrigel substrate or on polyacrylamide gels coated with laminin-1 or fibronectin. Cells were cultured for 48 h and RNA was then prepared using Trizol reagent (Invitrogen) according to the manufacturer's instructions, including an additional 10-min postlysis spin at 4°C to remove excess Matrigel if necessary. cDNA was prepared, and real-time PCR was performed as described elsewhere (31). Parallel PCR reactions were performed with ubiquitin C primers as a normalization control (32). All samples were run in triplicate using fibronectin primers from separate exons to eliminate potential contributions from genomic DNA: 5′-AAACTTGCATCTG-GAGGCAAACCC-3′ (forward) and 5′-AGCTCTGATCAGCATGGACCACTT-3′(reverse). Data were analyzed using SDS 2.1 software (Applied Biosystems).

Statistical analyses

Statistics were performed, and *P* values were calculated using a standard *t* test or a *t* test of proportions as appropriate. *P* values of <0.05 were considered significant. On all graphs, an asterisk (*) indicates that the difference between the control and treatment data is statistically significant. Graphs representing the percentage above the average of Matrigel control do not have error bars; however, the difference between them is statistically significant as determined above.

Results

Fibronectin is down-regulated during acinar morphogenesis

Whereas fibronectin production is high during development of the mammary gland (8), the normal, resting, adult mammary gland is largely devoid of fibronectin (13). To determine if

acinar morphogenesis of human MCF-10A cells mimics this down-regulation of fibronectin production seen *in vivo*, immunofluorescence staining of developing acini was used to qualitatively assess fibronectin production. During the early, proliferative stage of morphogenesis (days 1–7), fibronectin staining was evident circumferentially around the basal cell surface (Fig. 1*B*). However, in the late stages after growth arrest (days 15 and 21 acini), there was little to no fibronectin staining detectable. Decreased fibronectin was confirmed by examining fibronectin transcript and protein levels. Total cellular RNA isolated from cells grown on tissue culture plastic or Matrigel matrix for 48 hours was used for quantitative RT-PCR (qRT-PCR). Fibronectin transcript showed a nearly six-fold down-regulation on basement membrane matrix (Fig. 1*C*). Fibronectin production was determined by quantifying metabolically labeled protein secreted at different times of Matrigel culture. Three-fold more fibronectin was detected in the cell medium at the early time period, from 25 to 48 hours, compared with fibronectin produced between 72 and 96 hours on Matrigel matrix (Fig. 1*D*). These results show that fibronectin gene expression by MCF-10A cells is rapidly down-regulated, leading to reduced fibronectin secretion and matrix deposition as acinar morphogenesis progresses.

Fibronectin stimulates overproliferation and increases acinar size

Fibronectin is known to promote cell growth, so its down-regulation may be linked to the switch from proliferation to growth arrest as mammary epithelial cells differentiate. To test the effect of fibronectin on proliferation, high fibronectin levels were maintained by inclusion of excess rat fibronectin in the Matrigel matrix during differentiation. Proliferation of MCF-10A cells cultured with and without excess fibronectin was monitored during the initial proliferative phase of morphogenesis. Staining for expression of Ki-67, a nuclear antigen expressed from late G_1-M phase of the cell cycle, is a reliable indicator of cell cycle progression routinely used in this culture system (22,33–35). Cells were costained with DAPI, and the percentage of Ki-67–positive cells in the widest confocal cross-section of each acinus was calculated (Supplementary Fig. S1*A*). Most of the cells were positive for Ki-67 during the first few days on Matrigel and on Matrigel with excess fibronectin (day 1; Fig. 2*A*). However, the continuous presence of fibronectin maintained a significantly higher percentage of Ki-67–positive cells during days 4 to 7 compared with those grown on Matrigel matrix alone (Fig. 2A). The increased number of proliferating cells with excess fibronectin persisted throughout the growth phase, but the difference was negligible by day 9 with the onset of growth arrest. Cell shapes were indistinguishable on Matrigel with and without fibronectin. Immunofluorescence staining with anti-α5β1 integrin antibodies showed obvious basolateral staining of acini with and without fibronectin at 6 and 11 days of acinar development (data not shown).

To determine the effect of an increase in Ki-67–positive cells, cultures on Matrigel alone or with excess fibronectin were stained with DAPI to visualize nuclei (Supplementary Fig. S1*B*) and the number of cells in the widest confocal cross-section of each acinus was counted. The frequency of any given number of cells per acinus was then plotted, and the populations were compared with Gaussian fits (36). At days 12 and 20, well after the onset of growth arrest, the population grown on Matrigel with excess fibronectin was shifted to higher numbers of cells per acinus, relative to those grown on Matrigel alone (Fig. 2*B*). To determine if this change in size was statistically significant, the average cell number per acinus was calculated for the control cultures (Matrigel only, days 12 and 20) and the percentage of acini with more cells than the average of the Matrigel control was determined for Matrigel control and Matrigel with fibronectin cultures (Table 1A). These results show that when cultured in the presence of excess fibronectin, there is a statistically significant increase in the percentage of acini that are larger than the average of the Matrigel control (Table 1A; Fig. 2C). In addition to influencing acinar size, excess fibronectin resulted in a 50% decrease in the number of acini with no cells in the lumens compared with acini on Matrigel only. These data show a link between excess

fibronectin and increased proliferation of mammary epithelial cells resulting in a change in acinar size.

Introduction of fibronectin reverses growth arrest and affects acinar structure

Because fibronectin levels increase in the stroma of mammary tumors (13,14), this up-regulation may have an effect on mature acini. To recapitulate this situation, acini were allowed to differentiate on Matrigel alone before being confronted with exogenously provided fibronectin. Acini were cultured for 10 to 16 days, sufficient time for cells to exit the cell cycle and cease proliferation. At that time, medium was replaced with medium containing or lacking excess fibronectin, and Ki-67–positive cells were detected 2 and 4 days later. Cultures on Matrigel matrix exhibited a low level of proliferation, as expected for growth-arrested cells (Fig. 3A). In contrast, exposure to excess fibronectin induced a dramatic and rapid increase in the percentage of Ki-67–positive cells (8% versus almost 40% of total cells within 2 days). Renewed proliferation resulted in a persistent increase in cell number per acinus over the next 14 days. The size distribution of acini cultured on Matrigel with fibronectin is shifted to larger acinar size compared with those on Matrigel alone (Supplementary Fig. S2). After addition of fibronectin, the percentage of acini with above average cell numbers was significantly increased over control cultures at 2, 7, and 14 days (Table 1B; Fig. 3B). Another hallmark of acinar morphology is the presence of a hollow lumen. Introduction of fibronectin also decreased the percentage of acini with a hollow lumen (Supplementary Fig. S3A) with a parallel increase in the number of luminal cells (Supplementary Fig. S3B). These results show that introduction of fibronectin alters the growth-arrested state of mammary epithelial cells, increasing proliferation and cell number which encourages luminal filling.

Fibronectin promotes its own production

The negative effect of excess fibronectin during acinar development suggests that fibronectin down-regulation is essential for the normal morphogenetic process. To define the mechanism that underlies effects of fibronectin on morphogenesis, we investigated the ability of MCF-10A cells to down-regulate fibronectin production on Matrigel in the presence of extracellular fibronectin. Cells were plated on Matrigel matrix for 24 hours, at which time medium with or without fibronectin was added to the cultures and MCF-10A–produced protein was monitored by metabolic labeling. In cultures with exogenous fibronectin, newly synthesized fibronectin levels increased by 2-fold over parallel control cultures (Fig. 4A and B). Therefore, addition of fibronectin to cells growing on Matrigel matrix stimulates further fibronectin production, suggesting that fibronectin activates a positive-feedback loop to modulate its own expression.

This stimulation of fibronectin production is also apparent in late-stage acinar cultures. Acini were cultured on Matrigel or Matrigel with excess rat fibronectin for 21 days before being fixed and stained with DAPI and antihuman fibronectin antibodies (Fig. 4*C*). Average fibronectin fluorescence intensity of acini formed with excess fibronectin was significantly higher than those formed without fibronectin (Fig. 4*D*). No significant changes in α5β1 integrin levels were found in either early-stage or late-stage acini by fluorescence-activated cell sorting (FACS) or immunofluorescence, respectively (data not shown). These results show that continuous inclusion of fibronectin with Matrigel increases the amount of fibronectin matrix deposited within acini during MCF-10A differentiation.

Fibronectin expression is regulated by substrate composition and rigidity

During tumor formation in the breast, changes in tissue architecture and matrix composition are accompanied by increases in tissue rigidity. Relative to tissue culture plastic where MCF-10A fibronectin transcript levels were high, Matrigel is soft and fibronectin transcript levels were reduced by almost 6-fold (see Fig. 1*C*). In addition, fibronectin is the major ECM protein when MCF-10A cells are cultured on plastic, whereas Matrigel provides a laminin-rich

environment. To distinguish between the effects of ECM composition and rigidity, we used substrates of fibronectin or laminin-1 cross-linked to synthetic polyacrylamide gels of varying rigidity. Polyacrylamide gels were prepared with elastic moduli of 0.3 and 3.5 kPa, similar to Matrigel or normal mammary tissue and to mammary tumors, respectively (17). Gels at 34 kPa were used as a rigid control. The amount of ^{35}S-labeled fibronectin produced between 24 and 48 hours after plating was monitored. At 34 kPa, fibronectin production was reduced on the laminin-1 substrate compared with the fibronectin-coated gel (Fig. 5A and *B*), indicating that laminin-1, an abundant component of Matrigel, contributes to fibronectin down-regulation. Substrate rigidity also plays a role because cells on the 3.5-kPa gel produced less fibronectin than cells at 34 kPa. Interestingly, at 3.5 kPa, production of fibronectin by cells on laminin-1 was again lower than that by cells on fibronectin cross-linked gels (Fig. 5*A* and *B*). Cells produced similar low amounts of fibronectin when plated on the softest 0.3-kPa substrate, whether it was cross-linked with fibronectin or laminin-1. Overall, the differences between fibronectin levels on soft 0.3 kPa versus stiff 34 kPa substrates were 1.7-fold on laminin-1 and 2.5-fold on fibronectin (Fig. 5*B*). Fibronectin mRNA levels determined by qRT-PCR paralleled ^{35}S-protein levels (Fig. 5*C*). Furthermore, there was no difference in cell morphology on fibronectin relative to laminin-1 substrates at the same elastic modulus, and FACS analyses showed no difference in α5β1 integrin levels after 48 hours on polyacrylamide substrates with fibronectin or laminin at any rigidity (data not shown). These results show that a soft substrate is sufficient to down-regulate fibronectin production by MCF-10A cells. With increased matrix stiffness, contributions from the ECM, such as the presence of fibronectin, determine the level of fibronectin production.

Discussion

The data presented here identify fibronectin as an important effector of acinar morphogenesis. Down-regulation of fibronectin expression by MCF-10A cells is necessary for formation of spheric hollow acini, as inclusion of excess fibronectin stimulated cell growth and reversed established growth arrest of late-stage cultures. We also found that excess fibronectin induced MCF-10A cells to produce more fibronectin in a process that is affected by substrate rigidity. Thus, excess fibronectin perturbs both the acquisition and maintenance of acinar architecture by inducing cell proliferation, and this effect is likely to be exacerbated by increased production of fibronectin. These findings suggest that misregulation of fibronectin expression by transformed mammary epithelial cells *in vivo* may contribute to breast cancer progression by stimulating aberrant proliferation and loss of tissue architecture.

Previous work investigating the role of fibronectin in the mammary gland has correlated its expression with proliferation of epithelial cells. *In vivo* fibronectin and α5β1 expression and localization in epithelial cells of the intact gland correlate with periods of cell growth (8). Additionally, expression of a transgenic dominant-negative β1 integrin disrupted mammary gland development by decreasing proliferation and increasing apoptosis (37). *In vitro* mammary epithelial cells have been shown to respond to regulatory hormones when plated on fibronectin but not on laminin (38). Our results show that, during the initial stages of acinar differentiation on Matrigel, excess fibronectin increased proliferation. Early growth stimulatory effects have been linked to expression of a variety of signaling molecules, including human papillomavirus (HPV) E7 oncoprotein, ErbB2, cyclin D, and activated Akt (22,23, 33). Whereas HPV E7 and ErbB2 each induce sustained growth stimulation throughout morphogenesis, activated Akt, like fibronectin, has its primary proliferative effect in the early growth stage (23). Continuous activation of ErbB2 has a more dramatic effect than the others, causing significant overproliferation of MCF-10A cells into multiacinar structures with filled lumens (22,33). Together, these results show the differential effects on acinar morphogenesis of signaling through growth factor receptors, cell cycle pathways, and cell adhesion and

indicate that control of cell growth and growth arrest depends on the integration of multiple signals.

Signals from other matrix molecules are also essential because laminin-1 is needed to establish cell polarity and growth arrest (24). Laminin and laminin-binding integrins are well-known mediators of morphogenesis. Blocking β4 or β1 integrin function with antibodies perturbs acinar differentiation with effects including interruption of morphogenesis, inhibition of cell growth, and induction of apoptosis (21,34). Certainly, some of these effects are due to loss of laminin binding; however, our results suggest a reduction of interactions between α5β1 and fibronectin by anti-β1 function-blocking antibodies may also contribute. The dynamic nature of fibronectin production and its regulation by exogenous fibronectin during morphogenesis may provide new insights into mammary differentiation, development, and cancer progression. It is also interesting to speculate on the role fibronectin plays in branching morphogenesis in the breast as it is highly associated with epithelial cells during that process, and fibronectin has already been identified as an early signal inducing branching morphogenesis in the salivary gland (39).

During tumorigenesis in the breast, primary tumors are characterized by increased deposition of fibronectin (12–14,18,19), increased tissue rigidity (17), loss of epithelial cell polarity, increased proliferation, and luminal filling (1). Our data show that addition of excess fibronectin to differentiated cultures resulted in a reversal of growth arrest and failure to maintain the acinar structure. The reinitiation of cell growth and luminal filling seen here seem analogous to the changes seen with the emergence of breast cancer *in vivo*. Therefore, fibronectin may serve a key mitogenic role for mammary epithelial cells and promote oncogenic progression by stimulating aberrant proliferation.

Our results point toward a mechanism by which stiffening of the matrix affects proper acinar morphogenesis by modulating fibronectin expression. Conditions closest to those found in the normal mammary gland, laminin-rich with a low elastic modulus, favored down-regulation of fibronectin gene transcription, resulting in reduced protein production. In contrast, conditions similar to those found in mammary tumors, fibronectin-rich with a high elastic modulus, favored up-regulation of fibronectin mRNA and protein levels. Previous work has shown that progressively increasing the stiffness of the matrix prevents cells from differentiating into acini (17). Small increases in rigidity (0.1–4 kPa) resulted in increased proliferation and failure to form a hollow lumen, a phenotype similar to that seen for acini in the presence of excess fibronectin where epithelial cells are expressing high levels of fibronectin. This phenocopy and the increased fibronectin production on substrates with elastic moduli above that of Matrigel and normal mammary tissue may indicate that fibronectin contributes to the aberrant cell behaviors noted on stiff substrates.

Thus, in our model for fibronectin function during acinar morphogenesis, MCF-10A cells initially express fibronectin during the growth phase of differentiation. Over time, signals from Matrigel, including laminin-1 and low substrate rigidity, induce down-regulation of fibronectin, such that levels are negligible in fully differentiated, growth-arrested acini. This pattern is similar to that found *in vivo* in both mammary gland and lung (8,40). However, when the matrix is abnormal due to addition of exogenous fibronectin, a positive feedback loop is initiated, whereby fibronectin levels during the proliferative phase of morphogenesis are not reduced even after the onset of growth arrest, possibly contributing to the failure of acini in these circumstances to form a hollow lumen.

Modulation of fibronectin expression by tissue stiffness and the effects of increased fibronectin on cell growth may together have profound implications for breast cancer progression. It is understood that dense breast tissue, which is more rigid than normal tissue, is also prone to

development of hyperplasias and dysplasias (16,41). Should the altered stiffness of the mammary tissue promote increased fibronectin production by mammary epithelial cells, this would further stimulate proliferation. Indeed, a direct correlation was observed between mammographic density, deposition of the ECM proteoglycans lumican and decorin, and the presence of hyperplastic lesions (41). The propensity for hyperplastic growths to form in dense breast tissue may be in part due to increased deposition of fibronectin by mammary epithelial cells, which our results show can stimulate further fibronectin production and proliferation.

These data lend themselves to a model for the promotion of breast cancer progression by fibronectin (Supplementary Fig. S4). Oncogenic mutations in the mammary epithelium often result in a failure to maintain the basement membrane. This failure could then initiate a desmoplastic response, characterized by increased and aberrant deposition of ECM molecules (42) which would increase the elastic modulus of the tissue. Decreased contact with basement membrane laminin-1, increased contact with stromal fibronectin, and higher substrate rigidity may then stimulate mammary epithelial cells to produce their own fibronectin. Activation of this positive feedback loop would stimulate cell proliferation, leading to luminal filling and loss of normal tissue architecture. Thus, fibronectin may promote primary tumor formation by modifying the ECM to provide a substratum permissive for aberrant cell growth, thereby encouraging the acquisition of further oncogenic mutations.

Supplementary Material

Refer to Web version on PubMed Central for supplementary material.

Acknowledgments

Grant support: NIH R01 GM059383 and P01 CA41086 (J.E. Schwarzbauer); NIH T32 GM07388 Genetics and Molecular Biology training grant (Princeton University) and New Jersey Commission on Cancer Research predoctoral fellowship (C.M. Williams); and NIH T32 CA009528 (Princeton University; A.J. Engler).

We thank Dr. Stella Karuri for valuable assistance in statistical analyses and Dr. Peter Yurchenco for supplying purified laminin-1.

The HFN 7.1 antibody developed by R.J. Klebe was obtained from the Developmental Studies Hybridoma Bank developed under the auspices of the National Institute of Child Health and Human Resources and maintained by University of Iowa Department of Biological Sciences.

References

1. Nelson CM, Bissell MJ. Of extracellular matrix, scaffolds, and signaling: Tissue architecture regulates development, homeostasis, and cancer. Annu Rev Cell Dev Biol 2006;22:287–309. [PubMed: 16824016]
2. Stoker AW, Hatier C, Bissell MJ. The embryonic environment strongly attenuates v-src oncogenesis in mesenchymal and epithelial tissues, but not in endothelia. J Cell Biol 1990;111:217–228. [PubMed: 2164029]
3. van Roozendaal KE, Klijn JG, van Ooijen B, et al. Differential regulation of breast tumor cell proliferation by stromal fibroblasts of various breast tissue sources. Int J Cancer 1996;65:120–125. [PubMed: 8543388]
4. Deng G, Lu Y, Zlotnikov G, Thor AD, Smith HS. Loss of heterozygosity in normal tissue adjacent to breast carcinomas. Science 1996;274:2057–2059. [PubMed: 8953032]
5. Forsti A, Louhelainen J, Soderberg M, Wijkstrom H, Hemminki K. Loss of heterozygosity in tumour-adjacent normal tissue of breast and bladder cancer. Eur J Cancer 2001;37:1372–1380. [PubMed: 11435067]
6. Engbring JA, Kleinman HK. The basement membrane matrix in malignancy. J Pathol 2003;200:465–470. [PubMed: 12845613]

7. Aszodi A, Legate KR, Nakchbandi I, Fassler R. What mouse mutants teach us about extracellular matrix function. Annu Rev Cell Dev Biol 2006;22:591–621. [PubMed: 16824013]
8. Woodward TL, Mienaltowski AS, Modi RR, Bennett JM, Haslam SZ. Fibronectin and the α(5)β(1) integrin are under developmental and ovarian steroid regulation in the normal mouse mammary gland. Endocrinology 2001;142:3214–3222. [PubMed: 11416044]
9. Ronnov-Jessen L, Petersen OW, Bissell MJ. Cellular changes involved in conversion of normal to malignant breast: importance of the stromal reaction. Physiol Rev 1996;76:69–125. [PubMed: 8592733]
10. Sakakura T. New aspects of stroma-parenchyma relations in mammary gland differentiation. Int Rev Cytol 1991;125:165–202. [PubMed: 2032784]
11. Kadar A, Tokes AM, Kulka J, Robert L. Extracellular matrix components in breast carcinomas. Semin Cancer Biol 2002;12:243–257. [PubMed: 12083854]
12. Vasaturo F, Sallusti E, Gradilone A, et al. Comparison of extracellular matrix and apoptotic markers between benign lesions and carcinomas in human breast. Int J Oncol 2005;27:1005–1011. [PubMed: 16142317]
13. Christensen L. The distribution of fibronectin, laminin and tetranectin in human breast cancer with special attention to the extracellular matrix. APMIS Suppl 1992;26:1–39. [PubMed: 1576006]
14. Koukoulis GK, Howeedy AA, Korhonen M, Virtanen I, Gould VE. Distribution of tenascin, cellular fibronectins and integrins in the normal, hyperplastic and neoplastic breast. J Submicrosc Cytol Pathol 1993;25:285–295. [PubMed: 7686813]
15. Paszek MJ, Weaver VM. The tension mounts: mechanics meets morphogenesis and malignancy. J Mammary Gland Biol Neoplasia 2004;9:325–342. [PubMed: 15838603]
16. Boyd NF, Jensen HM, Cooke G, Han HL. Relationship between mammographic and histological risk factors for breast cancer. J Natl Cancer Inst 1992;84:1170–1179. [PubMed: 1635085]
17. Paszek MJ, Zahir N, Johnson KR, et al. Tensional homeostasis and the malignant phenotype. Cancer Cell 2005;8:241–254. [PubMed: 16169468]
18. Hao X, Sun B, Hu L, et al. Differential gene and protein expression in primary breast malignancies and their lymph node metastases as revealed by combined cDNA microarray and tissue microarray analysis. Cancer 2004;100:1110–1122. [PubMed: 15022276]
19. Yao ES, Zhang H, Chen YY, et al. Increased β1 integrin is associated with decreased survival in invasive breast cancer. Cancer Res 2007;67:659–664. [PubMed: 17234776]
20. Debnath J, Muthuswamy SK, Brugge JS. Morphogenesis and oncogenesis of MCF-10A mammary epithelial acini grown in three-dimensional basement membrane cultures. Methods 2003;30:256–268. [PubMed: 12798140]
21. Howlett AR, Bailey N, Damsky C, Petersen OW, Bissell MJ. Cellular growth and survival are mediated by β1 integrins in normal human breast epithelium but not in breast carcinoma. J Cell Sci 1995;108:1945–1957. [PubMed: 7544798]
22. Muthuswamy SK, Li D, Lelievre S, Bissell MJ, Brugge JS. ErbB2, but not ErbB1, reinitiates proliferation and induces luminal repopulation in epithelial acini. Nat Cell Biol 2001;3:785–792. [PubMed: 11533657]
23. Debnath J, Walker SJ, Brugge JS. Akt activation disrupts mammary acinar architecture and enhances proliferation in an mTOR-dependent manner. J Cell Biol 2003;163:315–326. [PubMed: 14568991]
24. Gudjonsson T, Ronnov-Jessen L, Villadsen R, Rank F, Bissell MJ, Petersen OW. Normal and tumor-derived myoepithelial cells differ in their ability to interact with luminal breast epithelial cells for polarity and basement membrane deposition. J Cell Sci 2002;115:39–50. [PubMed: 11801722]
25. Park CC, Zhang H, Pallavicini M, et al. β1 integrin inhibitory antibody induces apoptosis of breast cancer cells, inhibits growth, and distinguishes malignant from normal phenotype in three dimensional cultures and *in vivo*. Cancer Res 2006;66:1526–1535. [PubMed: 16452209]
26. Engvall E, Ruoslahti E. Binding of soluble form of fibroblast surface protein, fibronectin, to collagen. Int J Cancer 1977;20:1–5. [PubMed: 903179]
27. Mao Y, Schwarzbauer JE. Stimulatory effects of a three-dimensional microenvironment on cell-mediated fibronectin fibrillogenesis. J Cell Sci 2005;118:4427–4436. [PubMed: 16159961]

28. Wierzbicka-Patynowski I, Mao Y, Schwarzbauer JE. Continuous requirement for pp60-Src and phosphopaxillin during fibronectin matrix assembly by transformed cells. J Cell Physiol 2007;210:750–756. [PubMed: 17187346]
29. Engler AJ, Griffin MA, Sen S, Bonnemann CG, Sweeney HL, Discher DE. Myotubes differentiate optimally on substrates with tissue-like stiffness: pathological implications for soft or stiff microenvironments. J Cell Biol 2004;166:877–887. [PubMed: 15364962]
30. Pelham RJ Jr, Wang Y. Cell locomotion and focal adhesions are regulated by substrate flexibility. Proc Natl Acad Sci U S A 1997;94:13661–13665. [PubMed: 9391082]
31. Galante LL, Schwarzbauer JE. Requirements for sulfate transport and the diastrophic dysplasia sulfate transporter in fibronectin matrix assembly. J Cell Biol 2007;179:999–1009. [PubMed: 18056413]
32. Vandesompele J, De Preter K, Pattyn F, et al. Accurate normalization of real-time quantitative RT-PCR data by geometric averaging of multiple internal control genes. Genome Biol 2002;3:1–12.
33. Debnath J, Mills KR, Collins NL, Reginato MJ, Muthuswamy SK, Brugge JS. The role of apoptosis in creating and maintaining luminal space within normal and oncogene-expressing mammary acini. Cell 2002;111:29–40. [PubMed: 12372298]
34. Weaver VM, Petersen OW, Wang F, et al. Reversion of the malignant phenotype of human breast cells in three-dimensional culture and in vivo by integrin blocking antibodies. J Cell Biol 1997;137:231–245. [PubMed: 9105051]
35. Boudreau N, Werb Z, Bissell MJ. Suppression of apoptosis by basement membrane requires three-dimensional tissue organization and withdrawal from the cell cycle. Proc Natl Acad Sci U S A 1996;93:3509–3513. [PubMed: 8622967]
36. Zicha D, Genot E, Dunn GA, Kramer IM. TGFβ1 induces a cell-cycle-dependent increase in motility of epithelial cells. J Cell Sci 1999;112:447–454. [PubMed: 9914157]
37. Faraldo MM, Deugnier MA, Lukashev M, Thiery JP, Glukhova MA. Perturbation of β1-integrin function alters the development of murine mammary gland. EMBO J 1998;17:2139–2147. [PubMed: 9545227]
38. Haslam SZ, Woodward TL. Reciprocal regulation of extracellular matrix proteins and ovarian steroid activity in the mammary gland. Breast Cancer Res 2001;3:365–372. [PubMed: 11737887]
39. Sakai T, Larsen M, Yamada KM. Fibronectin requirement in branching morphogenesis. Nature 2003;423:876–881. [PubMed: 12815434]
40. Roman J, McDonald JA. Expression of fibronectin, the integrin α5, and α-smooth muscle actin in heart and lung development. Am J Respir Cell Mol Biol 1992;6:472–480. [PubMed: 1533775]
41. Alowami S, Troup S, Al-Haddad S, Kirkpatrick I, Watson PH. Mammographic density is related to stroma and stromal proteoglycan expression. Breast Cancer Res 2003;5:R129–R135. [PubMed: 12927043]
42. Walker RA. The complexities of breast cancer desmoplasia. Breast Cancer Res 2001;3:143–145. [PubMed: 11305947]

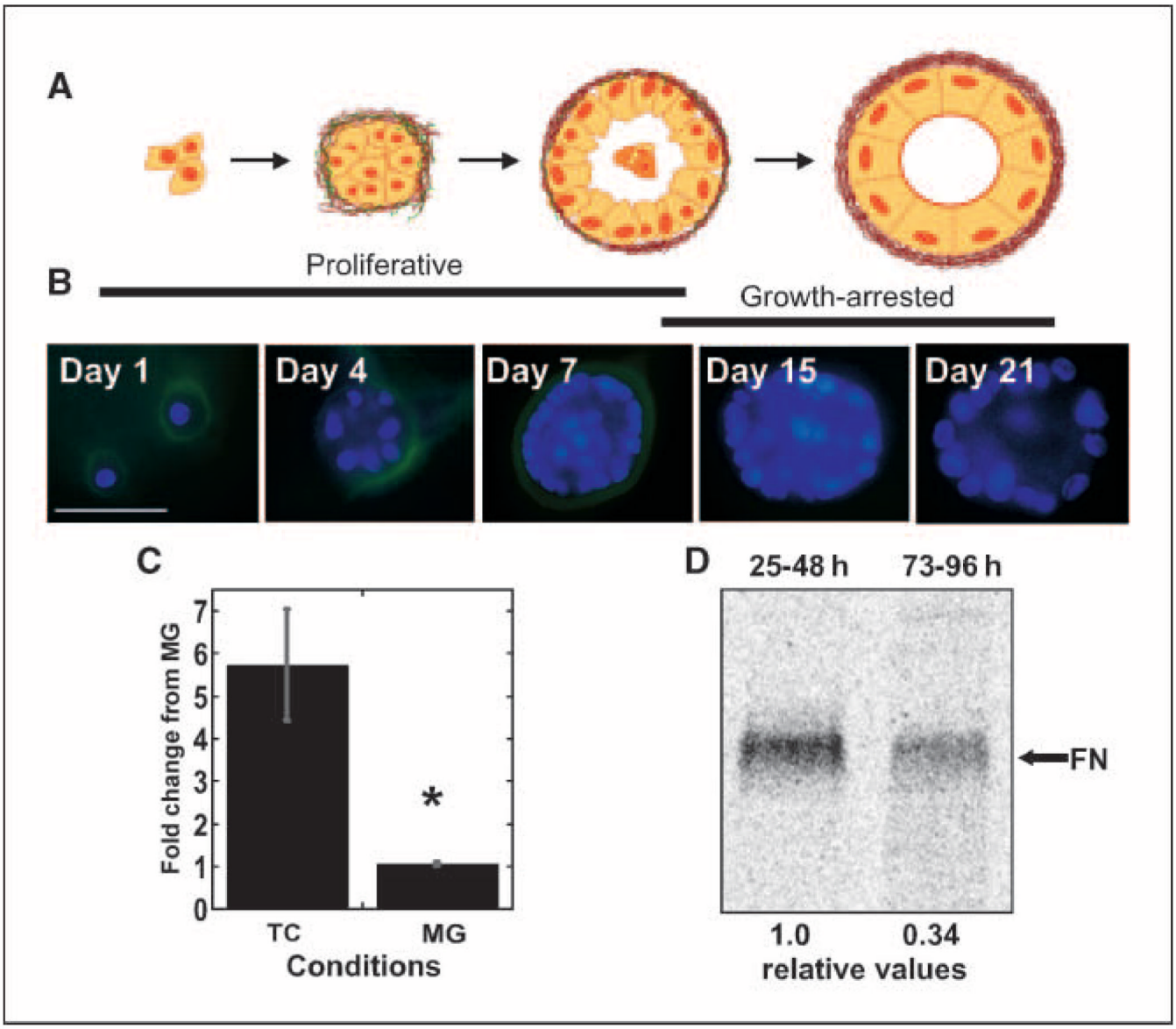

Figure 1.

Fibronectin is down-regulated during acinar morphogenesis. *A*, the stages of MCF-10A cell differentiation into a spherical hollow acinus are shown in this cartoon. *B*, MCF-10A mammary epithelial cells were stained with DAPI (blue) and with HFN7.1 antihuman fibronectin antibodies (*green*) at increasing times of development. Representative images for different days of development are shown. Cell proliferation and initiation of basement membrane formation, including fibronectin deposition, occur over the first 7 d on Matrigel reconstituted basement membrane matrix. After day 7, the cells growth arrest, become polarized, and undergo apoptosis to form a hollow lumen. Fibronectin staining decreases during this phase. *C*, cells were plated on tissue culture plastic or Matrigel (*MG*) matrix for 48 h before total cellular RNA was isolated and transcript levels were quantified by real-time RT-PCR. PCR products were normalized to levels of ubiquitin C transcript and graphed relative to levels in Matrigel samples. Graph represents the average of two independent experiments. *, $P < 0.04$. *D*, cells were labeled with [^{35}S]methionine for 24 h after 24 or 72 h of culture on Matrigel matrix. Fibronectin was affinity-purified from cell culture media; amounts from equivalent

numbers of cells were separated by SDS-PAGE and detected with a phosphor storage system. Relative fibronectin counts produced by cells on Matrigel from 24 to 48 h (set to 1.0) and 72 to 96 h are given below the lanes and represent the average of four independent experiments.

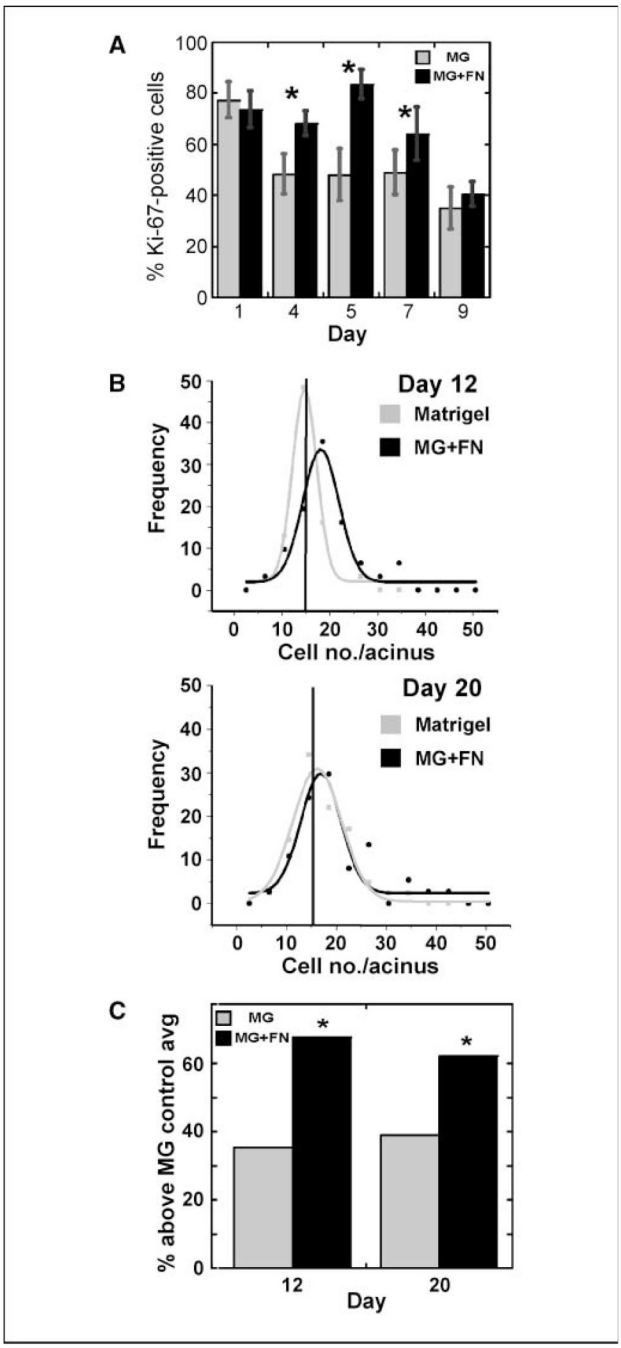

Figure 2.

Continuous presence of fibronectin increases proliferation and acinar cell number. *A*, Ki-67–positive cells were counted, and percentages were calculated at increasing times of culture on Matrigel without (*gray*) or with excess fibronectin (black). Between 100 and 400 cells were examined per condition. *, $P < 0.05$. B, the number of cells in populations of acini cultured on Matrigel alone (*gray*) or Matrigel with fibronectin (*MG + FN*, *black*) were counted after 12 and 20 d of differentiation. A bin size of 4 was used to plot the data, and the curves were fitted to the data with a Guassian equation. The results are representative of two experiments with at least 30 acini per condition per experiment. *Vertical line*, average number of cells per acinus for the population grown on Matrigel alone. Note that, unlike the Matrigel plot, the frequency

in the MG + FN plot does not go down to zero at the higher cell numbers. *C*, using the data presented in *A*, the percentage of acini with more cells than the average of the Matrigel control is graphed for cells plated on Matrigel or Matrigel with fibronectin. *, $P < 0.05$ by a t test of proportions.

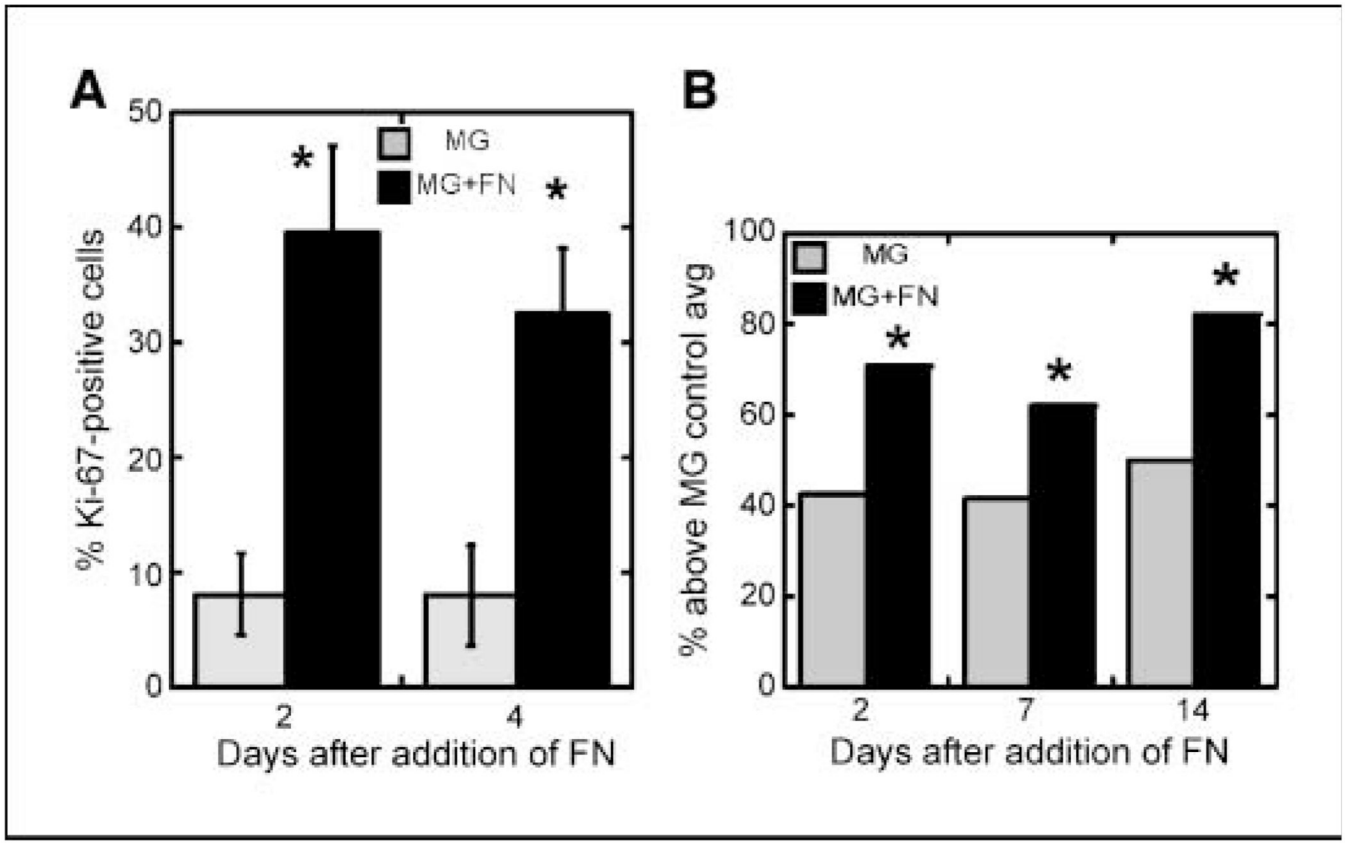

Figure 3.

Introduction of fibronectin into differentiated cultures reverses growth arrest. *A*, after 10 d in three-dimensional culture, medium was replaced with medium containing or lacking 50 μg/mL of rat fibronectin. Cultures were fixed and stained with DAPI and anti–Ki-67 antibody 2 or 4 d later. Percentage of Ki-67–positive cells was calculated. Between 150 and 250 cells were examined per condition per experiment. Results are representative of three independent experiments. *, $P < 0.05$. *B*, using the data presented in Supplementary Fig. S2, the percentage of acini with more cells than the Matrigel control's average is graphed for cells with Matrigel alone or Matrigel with fibronectin. *, $P < 0.05$ by a *t* test of proportions.

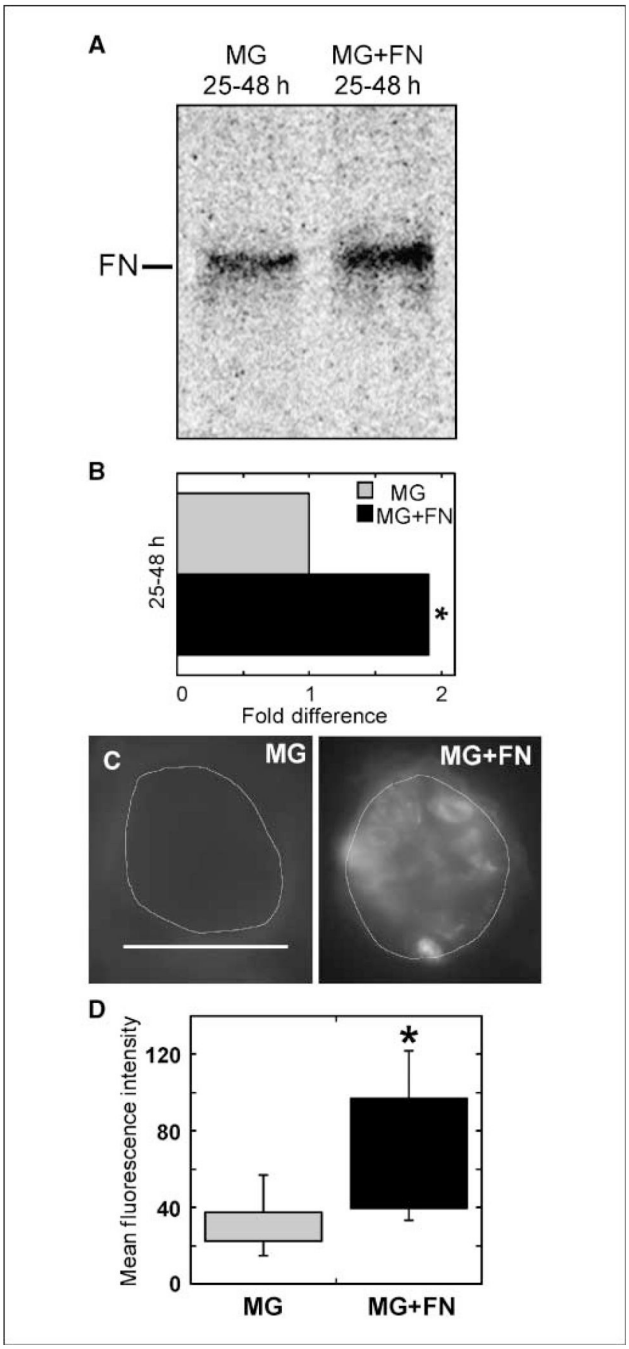

Figure 4.

Exogenous fibronectin increases endogenous fibronectin matrix deposition. *A*, cells were plated on Matrigel matrix for 24 h. Medium was exchanged for normal assay medium containing [^{35}S]methionine either without or with 50 μg/mL rat fibronectin. After an additional 24 h (25–48 h), culture medium was collected and fibronectin was analyzed as described in Fig. 1*D*. B, phosphor storage counts from Matrigel with excess fibronectin were normalized to Matrigel only, and the average fold change in extracellular fibronectin over 25 to 48 h is shown. Results are the average of four independent experiments. *, $P < 0.002$. *C*, representative images of MCF-10A acini formed on Matrigel matrix without or with 100 μg/mL rat fibronectin. Acini were permitted to differentiate for 21 d, then fixed, and stained with HFN7.1

antihuman fibronectin antibodies and DAPI. *Scale bar*, 50 μm. D, box plots representing all data points of fluorescence intensity of fibronectin staining are shown for acini developed on Matrigel or Matrigel with excess fibronectin. The middle 50% of the data points fall within the boxes, and the bars indicate the complete range of fluorescence intensities. $n = 18$ for MG and $n = 22$ for MG + FN. *, $P < 0.001$.

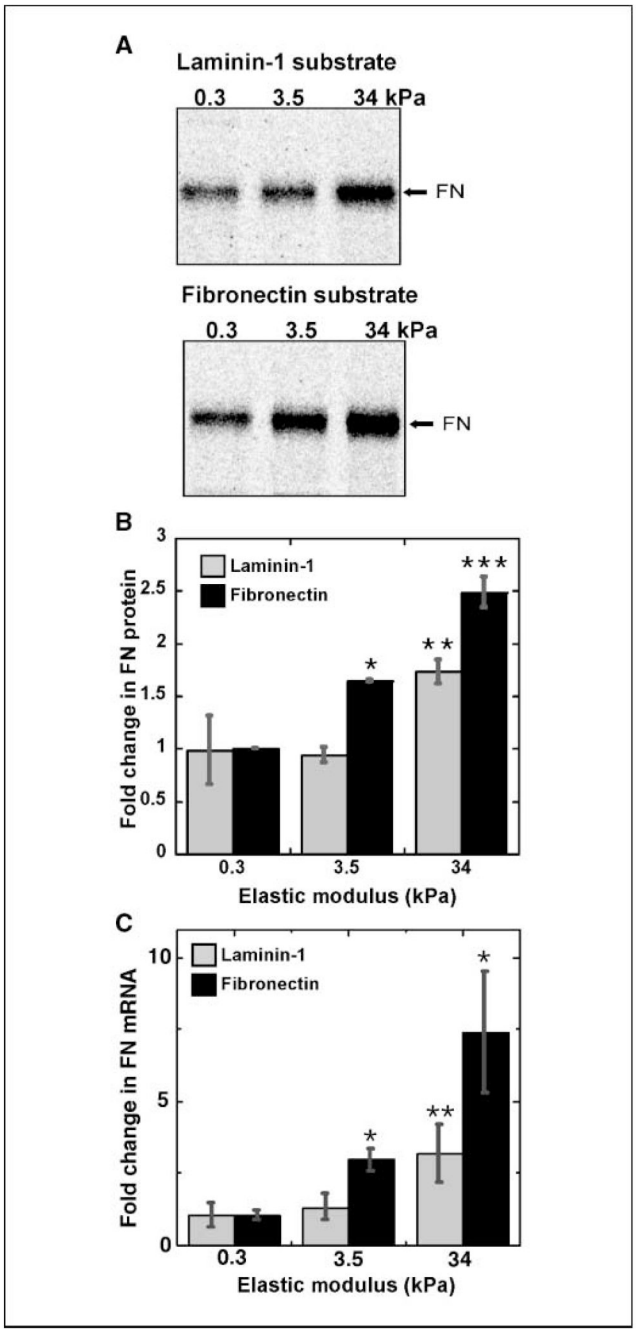

Figure 5.

Fibronectin expression is regulated by substrate rigidity and composition. *A*, cells were plated on fibronectin or laminin-1 cross-linked to polyacrylamide substrates with the indicated elastic moduli for 24 h, at which time coverslips were transferred to fresh medium containing [^{35}S] methionine. After an additional 24 h, samples were prepared and analyzed as in Fig. 1*D*. *B*, graph represents the average of phosphor storage counts from two independent experiments, presented as fold difference from fibronectin produced on fibronectin substrates at 0.3 kPa (set to 1.0). *, $P < 3$ times; 10^{-5}; **, $P < 0.004$; ***, $P < 0.002$. Additionally, the difference between laminin and fibronectin cross-linked substrates at 3.5 and 34 kPa is statistically significant ($P < 0.02$). C, real-time RT-PCR was performed on RNA isolated 48 h after cell plating on

fibronectin or laminin polyacrylamide gel substrates with indicated elastic moduli. Amounts of PCR products are presented as fold change relative to levels on 0.3 kPa fibronectin substrates. Graph represents the average of four independent experiments. *, $P < 0.05$; **, $P < 0.01$ compared with 0.3 kPa.

Table 1

Acinar sizes on Matrigel plus and minus fibronectin

A. Continuous fibronectin	**Day 12**		**Day 20**	
	MG	**MG + FN**	**MG**	**MG + FN**
Average no. cell per acinus	15.1		16.2	
Total no. acini	31	31	41	37
No. acini ≤ MG average	20	10	25	14
No. acini > MG average	11	21	16	23
% > MG average	35.5	67.7	39.0	62.2

B. Fibronectin reintroduction	**Day 2**		**Day 7**		**Day 14**	
	MG	**MG + FN**	**MG**	**MG + FN**	**MG**	**MG + FN**
Average no. cell per acinus	15.8		17.0		17.5	
Total no. acini	66	55	94	108	26	28
No. acini ≤ MG average	36	8	53	41	13	5
No. acini > MG average	30	47	41	67	13	23
% > MG average	45.5	85.5	43.6	62.0	50.0	82.1

Abbreviations: MG, Matrigel; MG + FN, Matrigel with fibronectin.